Design of Arrayed Waveguide Gratings in Silicon Nitride

B. Gargallo,[1] D. Doménech,[2] R. Baños,[1] D. Pastor,[1] C. Domínguez,[3] and P. Muñoz[1,2]

[1] iTEAM, Universitat Politècnica de València, Camino de Vera s/n, 46022 Valencia (Spain)
[2] VLC Photonics S.L., Camino de Vera s/n, 46022 Valencia (Spain)
[3] Institute of Microelectronics of Barcelona, IMB-CNM (CSIC), 08193 Bellatera (Spain)

In this paper the design and simulation of Arrayed Waveguide Gratings (AWGs) on Silicon Nitride (Si_3N_4) technology is reported. Comparison between 50, 100, 200 and 400 GHz AWGs is performed. The devices are being fabricated in a Si_3N_4 multi-project wafer (MPW) run using deeply etched waveguides and an orthogonal layout.

Introduction

Wavelength multiplexers are key components in almost every communication system using wavelength division multiplexing (WDM) techniques. There has been a lot of research in these components since the 90s, when WDM started to be an standard in telecom systems [1]. In this way, the Arrayed Waveguide Grating (AWG) [2] is one of the most important wavelength multi/demultiplexers, as it is a totally passive device that can be easily integrated in almost every technology. The AWG is not only used for WDM communication systems, but also in many other application fields, for instance as spectrometer fundamental block in sensing applications [3]. These other application domains may make use of wavelength ranges different from the typical used in communication applications. Hence, there is a growing interest of AWG applications in non-telecom wavelengths. For example, AWG-based systems for optical coherence tomography (OCT) [4, 5] or for the visible wavelength range [6] can be found in the literature. One of the most versatile photonic integration technologies is Silicon Nitride, since this material is transparent over a wide range of wavelengths, that from visible to the near infrared (400-2350 nm) [7]. Several Silicon Nitride platforms are in place and emerging, as for example LioniX [7], imec [8], IME [9] or CNM [10]. In this paper, we report the simulations and design of AWGs for the generic Si_3N_4 technology of CNM [10].

Technology

Silicon Nitride offers a lower index contrast in comparison with typical silicon-on-insulator (SOI) materials, which implies lower integration densities, at the advantage of reduced propagation loss and phase errors, being the latter a critical factor when designing interferometric devices as in the case of the AWG. It is important to remark that this technology also offers the possibility of designing devices for a wide wavelength range, being possible to guide the light from approximately 400 nm up to 2.3 μm. The technology employed for the designs is that of [10]. The Si_3N_4 structures are realized with CMOS compatible fabrication equipment and Low Pressure Chemical Vapor Deposition (LPCVD) processes. The lithography is carried out through a 365 nm line stepper and the waveguides are defined by conventional Reactive Ion Etching (RIE) processes. The fabrication process starts from 4 inch Silicon wafers that are partially oxidized (2.0 μm) and where a 300 nm thick Silicon Nitride layer is deposited through LPCVD. The basic waveguide geometry (deep waveguide) can be realized by a single lithography step, by fully etching

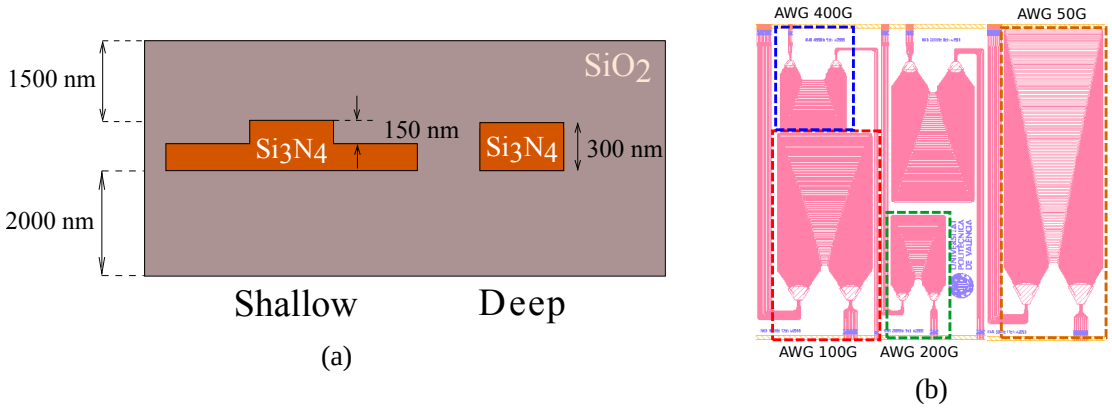

Figure 1: (a) Cross-sections for the shallow and deep waveguides in the CNM-VLC platform. (b) Designed mask for the AWG in the CNM platform.

Δf_{ch} [GHz]	N_{io}	FSR [nm]	N_{aw}	m	Δl [um]	L_f [um]
50	17	20.4	159	62	61.03	382.75
100	17	27.2	133	47	46.26	277.70
200	9	28.8	71	44	43.31	148.32
400	5	32.0	65	40	39.37	135.96

Table 1: AWG designed devices. Abbreviations: Δf_{ch} stands for the channel spacing, N_{io} for number of input/output waveguides, FSR for the free spectral range, N_{aw} for the number of arrayed waveguides, m for the grating order, Δl for the incremental length and L_f for the focal length.

the 300 nm layer of nitride. For the second type of waveguide available (shallow waveguide), just 150 nm of the guiding layer is etched. Finally the waveguides are covered with 1.5 μm of Silicon Oxide, deposited by Plasma Enhanced CVD (PECVD) technique. Figure 1a shows a schematic of the two waveguide cross-sections.

AWG design and simulations

The AWG is composed of one group of input waveguides connected to a first slab coupler or free propagation region (FPR). This first FPR is connected to a second one by means of a group of arrayed waveguides (AW), where consecutive waveguides lengths differ by a constant amount. Finally, the other side of the second FPR is connected to a group of output waveguides. Its functionality can be explained as follows: the field entering through one input waveguide is diffracted when it arrives to the first FPR, and this diffracted light is collected in the AWs. Due to the incremental length introduced in the AWs, when the light enters to the second FPR and is diffracted again, the different wavelengths have a constructive or destructive interference depending on the spatial position at the output. The output waveguides will be placed in the points where a constructive interference is obtained, having the different input wavelengths focused in the different output waveguides [11]. Regular AWGs with an orthogonal layout using waveguides with 2 μm width as input/outputs have been designed and simulated [11]. For this test devices, the targeted channel spacings are chosen to be the usual ones in communication systems: 50, 100, 200 and 400 GHz. A summary of all the designed devices is given in Table 1. Simulations of the waveguide cross-sections effective indices versus wavelength were performed us-

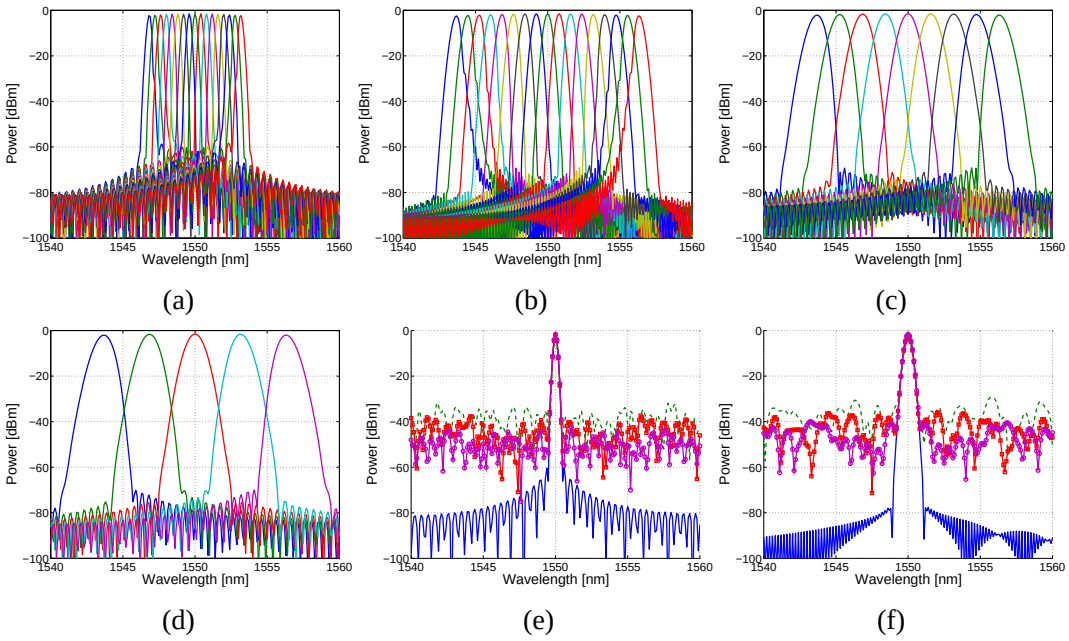

Figure 2: Simulations for the AWGs with different channel spacing: (a) 50 GHz, (b) 100 GHz, (c) 200 GHz and (d) 400 GHz. Simulations for the central channel in the (e) 50 GHz and (f) 100 GHz AWGs without phase errors (solid blue) and averaging 20 simulations with typical deviation a twentieth (magenta circled), a tenth (red squared) and a fifth part (green dashed) of the central wavelength inside the material.

ing a commercial software [12]. An effective index (n_{eff}) of 1.635 for the input/output waveguides with a 2.0 μm width and 1.575 for the 1.0 μm width cross-section were obtained. These will be used in the arrayed waveguides (AWs). Both indexes are calculated for the central wavelength (λ_c) of 1.55 μm. This AW width has been chosen to obtain monomode waveguides in the design wavelength range (C-band due to the availability of test equipment at our lab), but to be wider enough to minimize the phase errors associated to waveguides with a strong confinement [13], so as to minimize the induced spectral response distortions. Figure 1b shows the design mask including the four different AWGs using an orthogonal layout. In this case, only deep cross-sections have been used. The AWG simulations are shown in Fig. 2 for the four different channel spacings. The simulation losses are around 2 dB for every AWG designed. From simulations, it is possible to see that the outer channels start to be asymmetric, and this phenomena is more obvious in Figs. 2a and 2b, where the focal length is higher than in the other designs and the higher number of input/output waveguides causes a higher displacement from the central point where the aberrations will be zero. The main reason for this asymmetry is the use of the Rowland mounting for the slab couplers, which provokes aberrations when moving from the central point. These aberrations may be improved using other mounting as for example different focal points [14]. As was commented before, the phase error introduced in the arrayed waveguides due to fabrication is one of the critical factors in AWGs and it is related with the noise floor and the channel cross-talk. To obtain an approximation of the expected noise floor in the fabricated devices, simulations including these phase errors are performed. These errors will be introduced as a incremental/decremental length in the ar-

rayed waveguides, using normally distributed random lengths with a typical deviation that will be a fraction of the wavelength inside the material ($\sigma = \frac{\lambda_c}{n_{eff}N}$, with $N = [5, 10, 20]$) and mean equal to zero. As a result, Fig. 2(e)(f) shows the averaging of 20 simulations for the 50 and 100 GHz AWGs using different errors, providing a noise floor between -45 and -30 dB for the 50 GHz AWG and between -40 and -30 dB for the 100 GHz AWG.

Conclusion

The design and simulations of arrayed waveguide gratings in Silicon Nitride are presented in this paper. Different channel spacings have been chosen to test the fabrication process with regards to phase errors and induced spectral response distortion. These devices are currently being fabricated at the time of writing. Experimental results will be reported in the conference and/or future communications.

Acknowledgement

The authors acknowledge financial support by the Spanish MINECO project TEC2013-42332-P, acronym PIF4ESP, project FEDER UPVOV 10-3E-492 and project FEDER UPVOV 08-3E-008. B. Gargallo acknowledges financial support through FPI grant BES-2011-046100.

References

[1] C. A. Brackett, “Dense wavelength division multiplexing networks: principles and applications”, *IEEE J. Sel. Areas Commun.*, vol. 8(6), pp. 948–96, 1990.

[2] M. Smit and C. Van Dam, “PHASAR-based WDM-devices: Principles, design and applications”, *IEEE J. Sel. Topics Quantum Electron.*, vol. 2(2), pp. 236–250, 1996.

[3] T. Claes, W. Bogaerts, and P. Bienstman, “Vernier-cascade label-free biosensor with integrated arrayed waveguide grating for wavelength interrogation with low-cost broadband source”, *Opt. Lett.*, vol. 36(17), pp. 3320–3322, 2011.

[4] V. D. Nguyen e.a., “Spectral domain optical coherence tomography imaging with an integrated optics spectrometer”, *Opt. Lett.*, vol. 36(7), pp. 1293–1295, 2011.

[5] B. I. Akca e.a., “Toward Spectral-Domain Optical Coherence Tomography on a Chip”, *IEEE J. Sel. Topics Quantum Electron.*, vol. 18(3), pp. 1223–1233, 2012.

[6] B. Schauwecker e.a., “Small-Size Silicon-Oxynitride AWG Demultiplexer Operating Around 725 nm”, *IEEE Photon. Technol. Letters*, vol. 12(12), pp. 1645–1646, 2000.

[7] R. Heideman e.a., “Large-scale integrated optics using TriPleX waveguide technology: from UV to IR”, in *in SPIE Photonics West*, San Jose, CA, paper 7221-26, 2009.

[8] D. Martens e.a., “Compact Silicon Nitride Arrayed Waveguide Gratings for Very Near-Infrared Wavelengths”, *IEEE Photon. Technol. Letters*, vol. 27(2), pp. 137–140, 2015.

[9] L. Chen e.a., “Monolithic silicon chip with 10 modulator channels at 25 Gbps and 100-GHz spacing”, *Opt. Express*, vol. 19(26), pp. 946–951, 2011.

[10] D. Doménech e.a., “Generic silicon nitride foundry development: open access to low cost photonic integrated circuits prototyping”, in *9a Reunión Española de Optoelectrónica*, Salamanca, Spain, 2015.

[11] P. Muñoz, D. Pastor, and J. Capmany, “Modeling and design of arrayed waveguide gratings”, *J. Lightw. Technol.*, vol. 20(4), pp. 661–674, 2002.

[12] Optodesigner^{TM}, Phoenix Software BV, http://www.phoenixbv.com .

[13] W. Bogaerts e.a., “Silicon-on-Insulator Spectral Filters Fabricated With CMOS Technology”, *IEEE J. Sel. Topics Quantum Electron.*, vol. 16(1), pp. 33–44, 2010.

[14] D. Wang e.a., “Aberration Theory of Arrayed Waveguide Grating”, *J. Lightw. Technol.*, vol. 19(2), pp. 279–284, 2001.